Comparison of Fluorine-18-FDG PET and Thallium-201 SPECT in Evaluation of Lung Cancer

Kotaro Higashi, Takahiro Nishikawa, Hiroyasu Seki, Manabu Oguchi, Yoshihiro Nambu, Yoshimichi Ueda, Kokichi Yuasa, Hisao Tonami, Tetsuro Okimura and Itaru Yamamoto

Department of Radiology and Departments of Internal Medicine, Pathology and Thoracic Surgery, Kanazawa Medical University; and Department of Radiology, Kanazawa Cardiovascular Hospital, Ishikawa, Japan

We compared the diagnostic value of [^{18}F]2-fluoro-2-deoxy-D-glucose (FDG) PET imaging and ^{201}Tl SPECT imaging in the detection of primary lung cancer and mediastinal lymph node metastases. **Methods:** Thirty-three patients with histologically-proven primary lung cancer were examined with both FDG PET and Tl SPECT (early and delayed scans) within a week of each study. For semiquantitative analysis, the tumor-to-nontumor activity ratio (T-to-N ratio) was calculated. **Results:** Although both techniques delineated focal lesions with an increase in tracer accumulation in 28 patients, PET identified three additional patients in whom Tl SPECT images did not visualize any lesions on both early and delayed scans. In the detection of lung cancer of less than 2 cm in size, FDG PET provided higher sensitivity (six of seven, 85.7%) than did Tl SPECT early scan (one of seven, 14.3%) and delayed scan (four of seven, 57.1%). Neither technique visualized any lesions in two patients who had bronchioloalveolar carcinoma. The T-to-N ratio was significantly higher with FDG PET (10.39 ± 6.63) than it was with Tl SPECT (early scan, 2.37 ± 0.86; delayed scan, 3.01 ± 1.01) ($p < 0.0001$), whereas there was significant positive correlation between the FDG T-to-N ratio and the thallium T-to-N ratio ($p < 0.01$). Twenty-two patients had thoracotomies. Regarding the staging of mediastinal nodes, FDG PET detected mediastinal lymph node metastasis that was negative on Tl SPECT, whereas both techniques excluded tumor involvement in enlarged node at CT. **Conclusion:** Both techniques have clinical value for the noninvasive detection of primary lung cancer that is 2 cm or greater in diameter. However, if a PET camera is available, FDG PET is considered the method of choice for the evaluation of patients with suspected primary lung cancer that is less than 2 cm in diameter.

Key Words: PET; lung cancer; thallium-201; fluorine-18-fluorodeoxyglucose

J Nucl Med 1998; 39:9–15

Lung cancer is increasing in incidence throughout the world and is one of the major causes of death in many countries (*1*). The CT scan has played an important role in diagnosing and staging lung cancer. The spatial resolution of CT provides morphologic detail that is superior to that provided by other imaging techniques. However, CT has several limitations, including a limited ability to distinguish benign and malignant tumors (*2*). Recently, Swensen et al. (*3*) reported that lung nodule enhancement that is measured with CT is related to the likelihood of malignancy. Yamashita et al. (*4*) also stated that enhancement characteristics of lung cancers reflect the number of small tumoral vessels and the distribution of elastic fibers in the tumoral interstitium. However, not only lung cancer but also organizing pneumonia are enhanced significantly because the degree of enhancement at CT is related to the vascularity of the nodule (*5*).

Received Sep. 23, 1997; revision accepted Mar. 24, 1997.

For correspondence or reprints contact: Kotaro Higashi, MD, Department of Radiology, Kanazawa Medical University, 1-1, Daigaku, Uchinada, Kahoku-gun, Ishikawa, 920-02, Japan.

PET imaging with [^{18}F]2-fluoro-2-deoxy-D-glucose (FDG) has the potential value of delineating viable tumor tissue on the basis of increased glucose metabolism in the tumor. Recent reports indicated the value of FDG PET in diagnosing human lung cancer (*6–15*) and staging mediastinal nodes (*16–18*). However, the need for an expensive PET camera and cyclotron may limit the clinical application of this technique to patients with suspected lung cancer. Thallium-201 also has been used for the clinical diagnosis of lung cancer (*19–24*) and the detection of mediastinal lymph node metastasis from lung cancer (*25*). Accumulation of Tl was observed in viable tumor tissue (*26*), reflecting the proliferative potential of tumor cells (*27,28*) on the basis of Na^+-K^+ ATPase activity on the cell membrane (*29–31*). Tonami et al. (*19*) reported the value of Tl SPECT in detecting primary lung cancer and mediastinal lymph node metastases. FDG PET remains an expensive and complicated procedure, performed with tracers and imaging equipment that are available only at a limited number of sites. The technology needed to perform lung SPECT with Tl, on the other hand, is widely available, at only a fraction of the cost of PET. Few comparative studies between FDG PET and Tl SPECT have been reported (*32–36*). For these reasons, we performed a head-to-head comparison of these two scintigraphic examinations in patients with primary lung cancer to estimate their value in the detection of primary lung cancer and mediastinal lymph node metastases.

MATERIALS AND METHODS

Patients

Thirty-three patients (20 men and 13 women) with histologically-proven primary lung cancer participated in this study. Patient ages ranged from 42 yr to 82 yr, with a mean of 66 yr. Final diagnosis was established by histology (thoracotomy or bronchoscopy) in all patients. They consisted of 21 adenocarcinomas, 8 squamous cell carcinomas, 2 large cell carcinomas, 1 adenosquamous cell carcinoma and 1 small cell carcinoma. The size of the primary tumors was determined from the CT scans or the resected specimens and ranged from 1.2 cm to 9.5 cm. Twenty (60.6%) of the lung tumors were greater than 3 cm in diameter. Of the remaining 13 tumors, 6 were 2.0 cm–2.9 cm, and 7 were <1.9 cm. None of the patients had insulin-dependent diabetes, and serum glucose levels just before FDG injection were <120 mg/dl in all patients. Informed consent was obtained in all cases from patients who participated in the study.

Preparation of FDG

Fluorine-18 was produced by a ^{20}Ne(d,α)^{18}F nuclear reaction, and FDG was synthesized by the acetyl hydrofluorite method.

FDG PET

PET was performed using a PET camera (Headtom IV, Shimazu, Kyoto, Japan) that has four rings, providing seven tomographic slices. The intrinsic resolution was 5 mm FWHM at the center.

After at least 4 hr of fasting, each subject had transmission scanning for attenuation correction for 10 min. Immediately after the transmission scan, FDG was administered intravenously, and a static scan (14–24 tomographic slices at 6.5-mm intervals) was performed 40 min later for 10 min–20 min by using a 128 × 128 matrix. The average injection dose of FDG (radioactivity of preinjection syringe − radioactivity of postinjection syringe) was 178 MBq (4.8 mCi) and ranged from 104 MBq (2.8 mCi) to 318 MBq (8.6 mCi). The average injection dose of FDG in this study was approximately one-half of the dose that was reported previously (*7,8*). The effect of variance on the injection doses had been evaluated previously (*37*); therefore, no significant correlation was observed between the injection dose and the tumor-to-muscle radioactivity ratio, although the image quality and s.d. of the region of interest (ROI) data had deteriorated in the small injection dose. Here, body weights of the patients ranged from 39.2 kg to 75.0 kg, with a mean of 56.4 kg. The injection dose of FDG was reduced because of low body weight.

Thallium-201 SPECT

Within a week, all patients were examined with Tl SPECT. With the subjects at rest, 111 MBq (3 mCi) Tl-chloride were injected into a peripheral vein, and Tl imaging was begun 15 min (early scan) and 3 hr (delayed scan) later. SPECT was performed using a triple-headed rotating gamma camera system (PRISM 3000, Picker, Cleveland, OH), equipped with a high-resolution collimator, collecting 30 projection images for 40 sec each over 360° by using a 128 × 128 matrix. Total acquisition time was approximately 30 min. The intrinsic resolution was 15 mm FWHM at the center. The slice thickness was 5.8 mm. A series of transverse slices were reconstructed with filtered backprojection using a Ramp Hanning filter with a cutoff frequency of 0.5 cycles/pixel. No attenuation correction was performed.

CT Protocol

All patient had CT scanning of the chest before FDG PET and Tl SPECT imaging. CT scans were obtained with Helical CT system (TCT-900S/Super Helix; Toshiba, Tokyo, Japan). Contiguous 1-cm-thick sections were obtained at 1-cm intervals from the lung apices to the adrenal glands before and during intravenous bolus injection of contrast material at 2 ml/sec by means of a power injector.

Data Analysis

The FDG and Tl images were visually interpreted from the films by two readers and carefully correlated with contemporaneous CT study. For qualitative analysis, any obvious foci of increased FDG or Tl uptake over background were considered positive for tumor. For semiquantitative analysis of the FDG uptake, ROIs were placed over the most intense area of FDG accumulation. After correction for radioactive decay, the ROIs were analyzed by computing the standard uptake value (SUV) (tumor activity concentration/injected dose/body weight). The SUVs were calculated using a calibration factor between PET counts and radioactivity concentration. No recovery coefficient correction was applied. Activity ratios were calculated between the lesions and the homologous contralateral normal lung for an average tumor-to-nontumor activity ratio (T-to-N ratio). The activity ratios also are accurate methods of differentiating malignant and benign focal pulmonary abnormalities using FDG PET data analysis (*38*). On the other hand, for semiquantitative analysis of Tl SPECT, the radioactivity was measured for areas of the tumor showing the highest Tl accumulation and for the homologous contralateral normal lung to calculate the T-to-N ratio of the activity on early scan (early ratio, ER) and delayed scan (delayed ratio, DR). The retention index (RI) of Tl was also calculated for tumor activity according to the following equation: RI (%) = (DR − ER) × 100/ER.

Evaluation of Mediastinal Lymph Node Metastases

Twenty-two patients had thoracotomies, and the results of FDG PET, Tl SPECT and CT were compared with the pathologic findings of the mediastinal lymph nodes. CT scans were interpreted from film by two readers who were not aware of the PET and SPECT results. PET scans or SPECT scans also were interpreted at a later date by two readers who were also unaware of the previous CT interpretation. Nodes were measured along the short axis on the transverse CT imagings and were considered abnormal if they were ≥10 mm in short-axis diameter (*39*). Thallium-201 SPECT images were classified as positive for nodal involvement when there was at least one area of definitely increased radioactivity in the mediastinum, other than in the myocardium and thoracic spine. When there was no uptake of Tl in the mediastinum or when the accumulation was equivocal or could not be distinguished from that in the myocardium or vertebra, the images were considered negative. Foci of FDG uptake greater than mediastinal blood-pool activity were considered tumor, and foci of FDG uptake less than or equal to mediastinal blood-pool activity were considered nontumor. The SUV was not calculated for the mediastinum because of the problem of recovery coefficient and partial volume effects (*40*).

Statistical Analysis

Comparison of differences in FDG and Tl uptake was performed using the two-tailed Student's t-test for unpaired data. Probability values of less than 0.05 were considered to be statistically significant.

RESULTS

Table 1 summarizes the results of the radionuclide and pathological findings for the 33 patients studied.

Visual Analysis

FDG PET delineated focal lesions with an increase in tracer accumulation in 31 of 33 patients (93.9%) with primary lung cancer. The smallest tumor was 15 × 10 mm in size. On the other hand, Tl SPECT imaging showed an increase in tracer uptake in 23 of 33 patients (69.7%) on early scan and in 27 of 33 patients (81.8%) on delayed scan. FDG PET identified three additional patients in whom Tl SPECT images did not visualize any lesion on either early or delayed scans (Patients 12, 13 and 15). Two of these patients had adenocarcinoma of <2 cm in diameter (Patients 12 and 13). Another patient had adenocarcinoma that was 3.5 cm in size and localized near normal distribution of thallium in the myocardium (Patient 15). In the detection of lung cancer that was ≥2 cm in diameter, the sensitivities of Tl SPECT early scan (23 of 26, 88.5%) and delayed scan (23 of 26, 88.5%) were comparable to the sensitivity of FDG PET (25 to 26, 96.2%). A representative case is shown in Figure 1. In contrast, in the detection of lung cancer that is <2 cm in diameter, FDG PET provided higher sensitivity (six of seven, 85.7%) than did either Tl SPECT early scan (one of seven, 14.3%) or delayed scan (four of seven, 57.1%). A representative case is shown in Figure 2. Delayed scan of Tl SPECT provided higher sensitivity than did early scan. However, there was a patient in whom the lesion was visualized on early scan but not on delayed scan (Patient 7). Neither FDG PET nor Tl SPECT visualized any lesion in two patients who had bronchioloalveolar carcinoma (Patients 1 and 2). The sizes of these tumors were 1.2 cm and 2.2 cm.

Quantitative Analysis

Among the patients (n = 22) showing increased tracer accumulation, the T-to-N ratio of FDG PET ranged from 3.13 to

TABLE 1
Patient Characteristics and Radionuclide Imaging Results

Patient no.	Age (yr)	Sex	Histological type	Size (cm)	FDG T-to-N ratio	Tl ER	Tl DR
1	51	F	Bronchioloalveolar carcinoma	1.2 × 1.0	Negative	Negative	Negative
2	54	F	Bronchioloalveolar carcinoma	2.2 × 1.7	Negative	Negative	Negative
3	63	F	Bronchioloalveolar carcinoma	3.8 × 3.7	3.86	1.97	2.48
4	67	M	Bronchioloalveolar carcinoma	4.0 × 3.7	4.29	1.81	1.64
5	46	M	Adenocarcinoma	1.9 × 1.5	1.97	Negative	1.53
6	62	F	Adenocarcinoma	2.0 × 2.0	3.13	1.56	1.56
7	51	F	Adenocarcinoma	2.5 × 2.5	3.19	1.35	Negative
8	64	F	Adenocarcinoma	3.0 × 2.2	8.95	2.10	3.02
9	70	M	Adenocarcinoma	3.2 × 2.6	10.80	2.43	3.81
10	75	M	Adenocarcinoma	1.8 × 1.3	2.04	Negative	1.68
11	59	F	Adenocarcinoma	3.5 × 2.2	3.72	1.23	2.32
12	42	F	Adenocarcinoma	1.5 × 1.5	3.59	Negative	Negative
13	63	M	Adenocarcinoma	1.8 × 1.2	5.14	Negative	Negative
14	53	M	Adenocarcinoma	2.9 × 2.9	6.60	1.36	2.09
15	59	F	Adenocarcinoma	3.5 × 2.5	8.26	Negative	Negative
16	68	M	Adenocarcinoma	3.8 × 3.6	9.44	2.21	2.45
17	71	F	Adenocarcinoma	9.5 × 5.0	3.41	Negative	1.94
18	71	M	Adenocarcinoma	2.5 × 2.0	5.01	1.44	2.45
19	75	M	Adenocarcinoma	4.4 × 4.0	22.70	3.28	5.76
20	70	F	Adenocarcinoma	2.7 × 2.0	8.99	2.24	2.98
21	64	M	Adenocarcinoma	5.0 × 4.2	16.70	2.20	2.99
22	66	M	Squamous cell carcinoma	4.5 × 4.0	11.10	2.77	3.54
23	75	M	Squamous cell carcinoma	1.7 × 1.0	5.05	2.27	4.11
24	70	M	Squamous cell carcinoma	6.3 × 4.5	29.80	3.83	2.82
25	66	M	Squamous cell carcinoma	1.5 × 1.5	4.95	Negative	1.71
26	76	M	Squamous cell carcinoma	3.0 × 3.0	12.90	2.91	4.79
27	77	F	Squamous cell carcinoma	4.0 × 3.0	7.92	2.22	3.07
28	70	M	Squamous cell carcinoma	5.5 × 4.0	12.30	2.86	2.95
29	76	M	Squamous cell carcinoma	7.0 × 2.8	17.70	3.06	2.93
30	82	F	Large cell carcinoma	4.4 × 2.3	6.16	1.72	2.42
31	64	M	Large cell carcinoma	5.0 × 3.8	4.75	Negative	1.42
32	76	M	Adenosquamous cell carcinoma	3.1 × 3.1	8.21	1.78	2.01
33	72	M	Small cell carcinoma	4.8 × 3.0	13.30	2.02	4.02

29.8, with a mean of 10.39. Early ratio of Tl SPECT ranged from 1.23 to 4.79, with a mean of 2.37, and DR ranged from 1.56 to 5.76, with a mean of 3.01. The T-to-N ratio was significantly higher with FDG PET (10.39 ± 6.63) than it was with Tl SPECT (ER: 2.37 ± 0.86, $p < 0.0001$; DR: 3.01 ± 1.01, $p < 0.0001$) (Fig. 3). There were significant positive correlations between FDG T-to-N ratio and Tl ER ($r = 0.869$, $n = 23$, $p < 0.01$) (Fig. 4A) and between FDG T-to-N ratio and

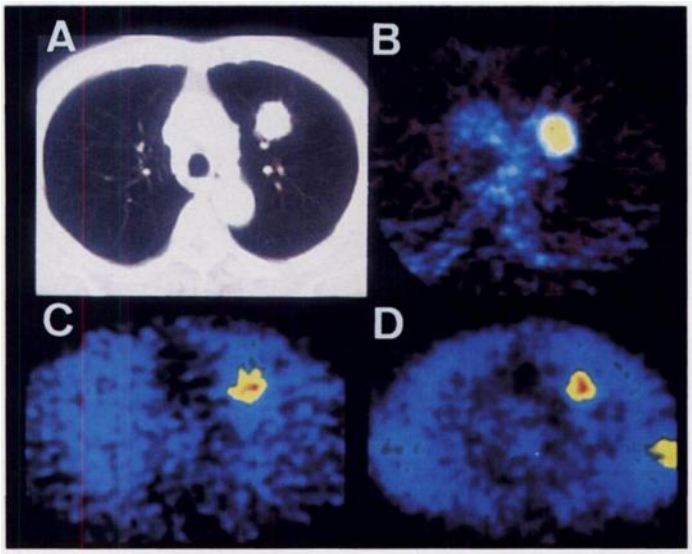

FIGURE 1. Patient 26, squamous cell carcinoma, 3.0 × 3.0 × 3.0 cm, pT1N0M0. (A) CT image shows nodule in the left lung. (B) FDG PET shows significantly hot accumulation in the tumor (SUV, 7.22; T-to-N ratio, 12.9). (C) Early scan on Tl SPECT. (D) Delayed scan on Tl SPECT. Tl SPECT also reveals good visualization of the tumor (ER, 2.91; DR, 4.79; RI, 64.6%).

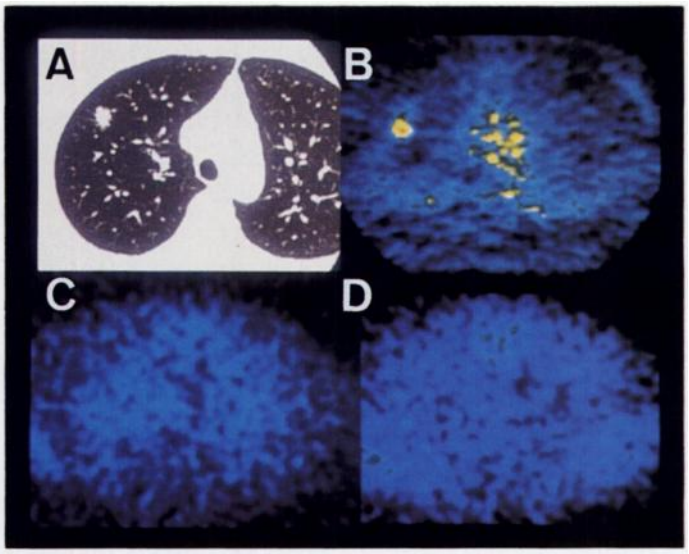

FIGURE 2. Patient 12, moderately differentiated tubular adenocarcinoma, 1.5 × 1.5 × 1.2 cm, pT1N0M0. (A) CT image shows nodule in the right lung. (B) FDG PET shows hot accumulation in the tumor (SUV, 2.64; T-to-N ratio, 3.59). (C) Early scan on Tl SPECT. (D) Delayed scan on Tl SPECT. Neither early nor delayed Tl SPECT visualized any lesions.

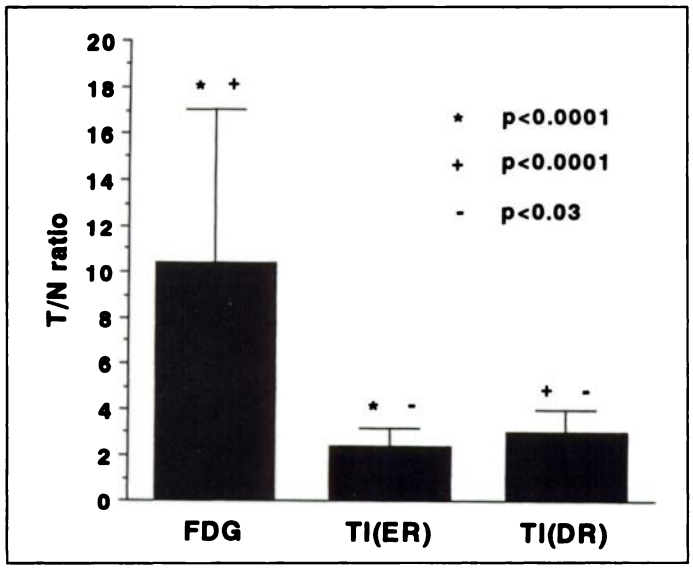

FIGURE 3. The T-to-N ratio was significantly higher with FDG PET (10.39 ± 6.63) than it was with Tl SPECT (ER, 2.37 ± 0.86; DR, 3.01 ± 1.01) ($p < 0.0001$).

DR ($r = 0.598$, $n = 27$, $p < 0.01$) (Fig. 4B), whereas there was no significant correlation between FDG T-to-N ratio and Tl RI ($r = 0.215$, $n = 22$, p value not significant). There were also significant positive correlations between FDG SUV and Tl ER ($r = 0.698$, $n = 23$, $p < 0.01$) and between FDG SUV and DR ($r = 0.526$, $n = 27$, $p < 0.01$), whereas there was no significant correlation between FDG SUV and Tl RI ($r = 0.118$, $n = 22$, p value not significant).

Detection of Mediastinal Lymph Node Metastases

Twenty-two patients with non-small cell lung cancer had thoracotomies, and tumor involvement of mediastinal lymph nodes was proven in 4 of 22 (18.2%) patients. FDG PET identified negative N2 nodes in 16 of 18 (88.9%) patients with negative nodes (Table 2). PET missed two of four nodal metastases. These nodes were <1 cm and had only microscopically tiny metastases (tumor emboli in peripheral sinus). Thallium-201 SPECT identified negative N2 nodes in 17 of 18 (94.4%) patients with negative nodes. Tl SPECT missed three of four nodal metastases. One was 1.7 × 1.0 cm, and the other nodes were <1 cm in diameter. CT missed three of four nodal metastases. These nodes were <1 cm in diameter. None of the techniques detected mediastinal lesions in two patients who had microscopically tiny metastases in normally sized lymph nodes.

TABLE 2
Comparative Performances of CT, Thallium-201 SPECT and FDG PET in Staging Mediastinal Lymph Node Metastases

	Mediastinal lymph node metastases	
	Positive	Negative
CT		
Positive	1	4
Negative	3	14
Tl SPECT		
Positive	1	1
Negative	3	17
FDG PET		
Positive	2	2
Negative	2	16

In one patient, FDG PET detected mediastinal lymph node metastases that were negative on Tl SPECT (Fig. 5). In one patient, both FDG PET and Tl SPECT detected a tumor in a normally-sized lymph node. In 18 patients without mediastinal lymph node metastases, four patients had lymphadenopathy on CT. In two of these patients, both FDG PET and Tl SPECT excluded tumor involvement in enlarged nodes at CT. Although false-positive results were somewhat common with CT, they occurred only occasionally with FDG PET and Tl SPECT. There were two false-positive cases, with a slight increase in FDG uptake (one hyperplasia of lymph follicle and one anthracotic node). Another false-positive case showed a slight increase in Tl uptake (hyperplasia of lymph follicle).

DISCUSSION

In the detection of lung cancer that is ≥2 cm in diameter, the sensitivities of Tl SPECT early scan (23 of 26, 88.5%) and delayed scan (23 of 26, 88.5%) were comparable to the sensitivity of FDG PET (25 of 26, 96.2%) (Fig. 1). In contrast, in the detection of lung cancer that is <2 cm in diameter, FDG PET provided higher sensitivity (six of seven, 85.7%) than did either Tl SPECT early scan (one of seven, 14.3%) or delayed scan (four of seven, 57.1%) (Fig. 2). The T-to-N ratio was 3–4 times higher with FDG PET than it was with Tl-SPECT (Fig. 3). Thus, FDG-PET provided better sensitivity for detecting lung cancer that is <2 cm in diameter and had a higher T-to-N ratio than did Tl SPECT. However, neither FDG PET nor Tl SPECT visualized any lesion in two patients who had bronchioloalveolar carcinoma. Scott et al. (*10*) reported that, based on visual inspection of the images, the FDG-PET scans correctly identified 44 of 47 pulmonary malignancies. Of the three

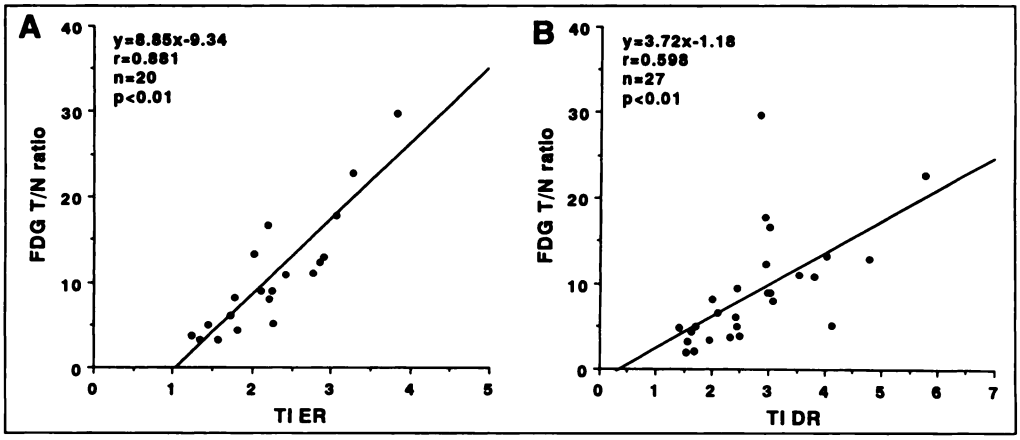

FIGURE 4. (A) Relationship between FDG T-to-N ratio and Tl ER. There was significant positive correlation between FDG T-to-N ratio and Tl ER ($r = 0.869$, $n = 23$, $p < 0.01$). (B) Relationship between FDG T-to-N ratio and Tl DR. There was significant positive correlation between FDG T-to-N ratio and Tl DR ($r = 0.598$, $n = 27$, $p < 0.01$).

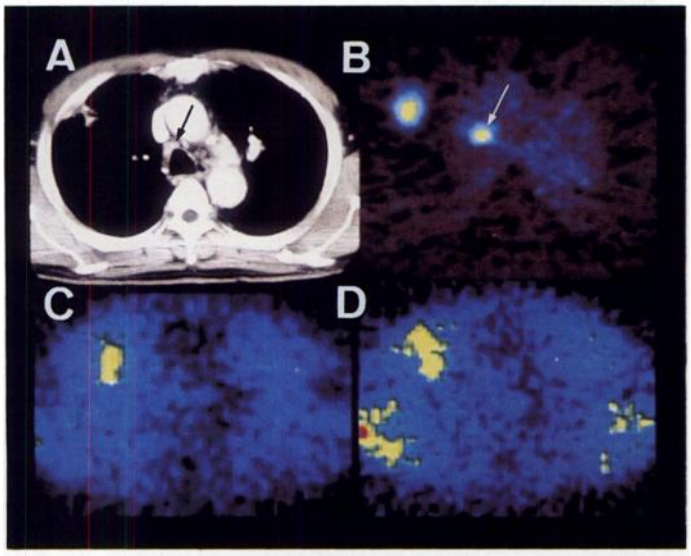

FIGURE 5. Patient 32, adenosquamous cell carcinoma, pT2N2M0. (A) Slightly enlarged right mediastinal lymph node (arrow) in a patient with a right lung primary lesion is seen on contrast-enhanced CT scan. (B) PET scan shows intense FDG uptake (arrow) by mediastinum 40 min after tracer injection. (C) Early scan on Tl SPECT. (D) Delayed scan on Tl SPECT. Neither early nor delayed Tl SPECT visualized any lesions. Metastatic cancer was proven in the right mediastinal nodes of this patient.

false-negative findings, two were for tumors that were <1 cm in diameter, and the other was for a bronchioloalveolar carcinoma. Thus, FDG PET scans correctly identified pulmonary malignancies that were >1 cm in diameter, except for bronchioloalveolar carcinomas. Tumors <1 cm in diameter were noted to be particularly difficult to evaluate because of their small size relative to the resolution of the PET scanner (*7*). In general, objects that are smaller than twice the resolution of the imaging system will show recovery coefficients that are substantially less than one (*40*).

Although Tl SPECT detected lung cancer in the majority of patients, the sensitivity of Tl SPECT was inferior to that of FDG PET in the detection of lung cancer that is <2 cm in diameter in our study. Tonami et al. (*41*) reported visualization of 147 (100%) malignant pulmonary lesions in 170 patients with suspected malignant pulmonary lesions that were >2 cm in diameter. Similarly, Suga et al. (*42*) evaluated 106 suspected malignant thoracic lesions that were >2 cm in diameter with Tl SPECT. All 48 (100%) malignant lesions were visualized on Tl SPECT. These authors concluded that the lack of thallium uptake in nodules that are >2 cm in diameter effectively excluded malignancy. Orihashi et al. (*43*) evaluated 40 pulmonary nodules between 1 cm and 3 cm in diameter with Tl SPECT. Two of three malignant lesions <2 cm in diameter were not visualized, whereas all malignant lesions that were >2 cm in diameter were visualized. These reports were consistent with our results.

Thallium-201 SPECT has another limitation that is due to its background uptake in muscle and myocardium, as seen in Figures 1 and 5. The background uptake in muscle may hinder determination of chest wall (rib/muscle) involvement. Thallium-201 uptake in myocardium may hinder the detection of lung cancer. In this study, one of three patients with positive FDG PET but negative Tl SPECT had lung cancer localized near the myocardium.

Several reasons for the discordance between FDG and Tl distributions are possible (*32*). First, the spatial resolutions and the sensitivities were strikingly different between PET and SPECT, which may cause a great difference in image quality (*44–46*). Martin et al. (*44*) compared FDG SPECT with FDG PET to evaluate malignancies. Sensitivities of PET and SPECT were 82.8 cpm/MBq and 4.8 cpm/MBq, respectively (reconstructed special resolutions, 7 and 17 mm, respectively). FDG SPECT detected 36 of 46 (78%) lesions that were depicted at FDG PET. In the detection of malignancies ≤1.8 cm in diameter, FDG PET provided higher sensitivity than did FDG SPECT. These results were similar to the results of our study comparing FDG PET and Tl SPECT, and it was suggested that Tl SPECT may be comparable to FDG SPECT in the detection of lung cancer. Second, the scintigraphic detectability depends not only on size of the lesion and degree of uptake of radiopharmaceutical but also on the contrast of the lesion uptake with surrounding tissues (*44*). Activity ratios between the lesions and the homologous contralateral normal lung (T-to-N ratios), on average, were higher with FDG PET (10.39 ± 6.63) than they were with Tl SPECT (ER, 2.37 ± 0.86; DR, 3.01 ± 1.01), and two lung cancers that were ≥5 cm in diameter were not depicted on early scan of Tl SPECT. A part of these phenomena may be attributed to increased Tl accumulation in the normal lung, especially on early scan of Tl SPECT. Third, the mechanisms of the accumulation of these tracers in tumors are different. FDG is transported, phosphorylated and metabolically trapped in tumor cells as FDG-6-phosphate. The mechanisms for increased FDG-6-phosphate accumulation in many cancer cells has been shown to be due to:

1. increased expression of glucose transporter molecules at the tumor cell surface;
2. increased level/activity of hexokinase; and
3. reduced levels of glucose-6-phosphatase compared to most normal tissues (*15*).

Thallium-201 uptake is considered to reflect the regional perfusion and viability of tumor cells (*20,21*). Regarding the mechanism of Tl accumulation in tumors, a relationship to Na^+-K^+ ATPase has been reported (*23,24*). Slosman et al. (*47*) reported that cell incorporation of Tl differed from that of [^{3}H]deoxyglucose in vitro, suggesting that it was not directly related to cell glycolysis activity. Oriuchi et al. (*35*) also showed that Tl uptake in glioma may be independent of increased glucose transport or metabolism, using comparative SPECT and PET studies. However, both FDG and Tl have been shown to be markers of viable tumor in autoradiographic studies (*26,48*). Here, there was a significant positive correlation between FDG uptake (SUV and T-to-N ratio) and Tl uptake (ER and DR) in primary lung cancer (Fig. 4A and B).

Another issue in lung cancer management is whether the tumor has spread to the mediastinal lymph nodes. This question is of substantial importance in non-small cell lung cancer, in which a cure is generally possible only with the complete excision of viable tumor from the thorax. Prospective data from the multi-institutional Radiologic Diagnostic Oncology Group trial (*2*) showed that, in staging non-small cell lung cancer, CT was only 52% sensitive and 69% specific, whereas MR imaging was 48% sensitive and 64% specific. Wahl et al. (*16*) reported that FDG PET was substantially more accurate than CT in staging presumed non-small cell lung cancer. In this prospective study of 23 patients, FDG PET was about 81% accurate, CT was 52% accurate ($p < 0.05$) and neither CT nor FDG PET was perfect in this clinical setting. However, FDG PET often had the capability to detect tumors in some normally-sized lymph nodes and exclude tumor involvement in enlarged lymph nodes. Yokoi et al. (*25*) compared Tl SPECT with CT in the detection of mediastinal lymph node metastases from lung cancer in 113 patients. The sensitivity of CT was 62%, and the specificity was

80%. These rates were higher for Tl SPECT (76% and 92%, respectively), and Tl SPECT was considered to be very helpful in facilitating prediction of the presence of mediastinal metastases in patients with enlarged nodes at CT. In our preliminary study, one patient had true-positive FDG PET and false-negative Tl SPECT (Fig. 5). FDG PET had the capability to detect mediastinal lymph node metastases that were negative on Tl SPECT. However, no techniques, including FDG PET, detected mediastinal lesion in two patients who had microscopically tiny metastases (tumor emboli in peripheral sinus) in normally-sized lymph nodes. This finding may be partly attributed to the phenomenon that FDG uptake is related to viable cancer cell number (*49*). Two patients had true-negative FDG PET and Tl SPECT and false-positive CT. FDG PET and Tl SPECT also had the capability to exclude tumor involvement in enlarged nodes at CT.

This study has several limitations. First, the number of patients who had pathologic staging of their mediastinal lymph nodes is limited. This study included only four patients with tumor involvement of mediastinal lymph nodes. Therefore, few conclusions can be drawn from these data regarding the ability of FDG PET imaging to detect mediastinal lymph node metastases. It is clear that additional study is essential. Second, both the PET and the SPECT are limited in this study in their ability to detect distant metastases, such as adrenal/liver involvement, which is a vital aspect of the staging of these patients with lung cancer, because of the "non"-whole-body mode of image acquisition. Third, this study included only cases of histologically proven lung cancer. Therefore, although the true-positive rate for these studies could be calculated, the true-negative rate could not be evaluated. In this respect, a prospective analysis of patients with suspected lung cancer may be warranted for comparing the diagnostic accuracy of these techniques.

CONCLUSION

In the detection of lung cancer that is ≥2 cm in diameter, the sensitivity of Tl SPECT was comparable to the sensitivity of FDG PET. Furthermore, there was significant positive correlation between FDG uptake and Tl uptake in primary lung cancer. Therefore, both techniques are considered to have clinical value for the noninvasive detection of primary lung cancer that is ≥2 cm in diameter. FDG PET, however, provided significantly higher sensitivity in patients with primary lung cancer that is <2 cm in diameter and higher contrast than Tl SPECT. If a PET camera is available, FDG PET is considered the method of choice for the evaluation of patients with suspected lung cancer that is <2 cm in diameter.

ACKNOWLEDGMENTS

We thank Nobuo Oya, MD, for helpful discussion. We also thank the PET technologists and PET chemistry staff of Kanazawa Cardiovascular Hospital for their contributions. This work was supported by a Grant for Collaborative Research (C95-2) and a Grant for Project Research (P96-2) from Kanazawa Medical University and by Grants-in-Aid for Scientific Research (07671031) from the Ministry of Education, Science and Culture, Japan.

REFERENCES

1. Stanley K, Stjernsward J. Lung cancer. In: Hansen HH, ed. *Basic and clinical concepts of lung cancer*. Norwell, MA: Kluwer; 1989:1–4.
2. Webb WR, Gatsonis C, Zerhouni EA, et al. CT and MR imaging in non-small cell bronchogenic carcinoma: report of the Radiologic Diagnostic Oncology Group. *Radiology* 1991;178:705–713.
3. Swensen SJ, Brown LR, Colby TV, Weaver AL. Pulmonary nodules: CT evaluation of enhancement with iodinated contrast material. *Radiology* 1995;194:393–398.
4. Yamashita K, Matsunobe S, Takahashi R, et al. Small peripheral lung carcinoma evaluated with incremental dynamic CT: radiologic–pathologic correlation. *Radiology* 1995;196:401–408.
5. Swensen SJ, Brown LR, Colby TV, et al. Lung nodule enhancement at CT: prospective finding. *Radiology* 1996;201:447–455.
6. Kubota K, Matsuzawa T, Fujiwara T, et al. Differential diagnosis of lung tumor with positron emission tomography: a prospected study. *J Nucl Med* 1990;31:1927–1933.
7. Gupta NC, Frank AR, Dewan NA, et al. Solitary pulmonary nodules: detection of malignancy with PET with 2-[F-18]-Fluoro-2-deoxy-D-glucose. *Radiology* 1992;184: 441–444.
8. Patz EF, Lowe VJ, Hoffman JM, et al. Focal pulmonary abnormalities: evaluation with F-18 fluorodeoxyglucose PET scanning. *Radiology* 1993;188:487–490.
9. Nolop KB, Rhodes CG, Brudine LH, et al. Glucose utilization in vivo by human pulmonary neoplasms. *Cancer* 1987;60:2682–2689.
10. Scott WJ, Schwabe JL, Gupta NC, Dewan NA, Reeb SD, Sugimoto JT. Positron emission tomography of lung tumors and mediastinal lymph nodes using [^{18}F]fluorodeoxyglucose. *Ann Thorac Surg* 1994;58:698–703.
11. Patz EF, Lowe VJ, Hoffman JM, Paine SS, Harris LK, Goodman PC. Persistent or recurrent bronchogenic carcinoma: detection with PET and 2-[F-18]-2-deoxy-D-glucose. *Radiology* 1994;191:379–382.
12. Rege SD, Hoh CK, Glaspy JA, et al. Imaging of pulmonary mass lesions with whole-body positron emission tomography and fluorodeoxyglucose. *Cancer* 1993;72: 82–90.
13. Dewan NA, Gupta NC, Redepenning LS, Phalen JJ, Frick NP. Diagnostic efficacy of PET-FDG imaging in solitary pulmonary nodules. *Chest* 1993;104:997–1002.
14. Gupta NC, Maloof J. Probability of malignancy in solitary nodules using fluorine-18-FDG and PET. *J Nucl Med* 1996;37:943–948.
15. Wahl RL. Positron emission tomography: applications in oncology. In: Murray IPC, Ell PJ, eds. *Nuclear medicine in clinical diagnosis and treatment*, Vol. 2. New York: Churchill Livingstone; 1994:801–820.
16. Wahl RL, Quint LE, Greenough RL, Meyer CR, White RI, Orringer MB. Staging of mediastinal non-small cell lung cancer with FDG PET, CT and fusion images: preliminary prospective evaluation. *Radiology* 1994;191:371–377.
17. Chin R Jr, Ward R, Keyes JW, et al. Mediastinal staging of non-small cell lung cancer (NSCLC) to compare its yield to that of computed tomography (CT). *Am J Respir Crit Care Med* 1995;152:2090–2096.
18. Sasaki M, Ichiya Y, Kuwabara Y, et al. The usefulness of FDG positron emission tomography for the detection of mediastinal lymph node metastases in patients with non-small cell lung cancer. *Eur J Nucl Med* 1996;23:741–747.
19. Tonami N, Shuke N, Yokoyama K, et al. Thallium-201 single photon emission computed tomography in the evaluation of suspected lung cancer. *J Nucl Med* 1989;30:997–1004.
20. Matsuno S, Tanabe M, Kawasaki Y, et al. Effectiveness of planar image and single photon emission tomography of thallium-201 compared with gallium-67 in patients with primary lung cancer. *Eur J Nucl Med* 1992;19:86–95.
21. Namba R, Narabayashi I, Matsui R, et al. Evaluation of Tl-201 SPECT for monitoring the treatment of pulmonary and mediastinal tumors. *Ann Nucl Med* 1995;9:65–74.
22. Itoh K, Takekawa H, Tsukamoto E, et al. Single photon emission computed tomography using ^{201}Tl chloride in pulmonary nodules: comparison with ^{67}Ga citrate and ^{99}mTc-labeled hexamethyl-propyleneamine-oxime. *Ann Nucl Med* 1992;6:253–260.
23. Abdel-Dayem HM, Scott A, Macapinlac H, Larson S. Tracer imaging in lung cancer. *Eur J Nucl Med* 1994;21:57–81.
24. Chin BB, Zukerberg BW, Buchpiguel C, Alavi A. Thallium-201 uptake in lung cancer. *J Nucl Med* 1995;36:1514–1519.
25. Yokoi K, Okuyama A, Nori K, Tominaga K, Miyazawa N, Takizawa I, Sasawaga M. Mediastinal lymph node metastasis from lung cancer: evaluation with Tl-201 SPECT. Comparison with CT. *Radiology* 1994;192:813–817.
26. Ando A, Ando I, Katayama M, et al. Biodistributions of Tl-201 in tumor-bearing animals and inflammatory lesion induced animals. *Eur J Nucl Med* 1987;12:567–572.
27. Ishibashi M, Taguchi A, Sugita Y, et al. Thallium-201 in brain tumors: relationship between tumor cell activity in astrocytic tumor and proliferating cell nuclear antigen. *J Nucl Med* 1995;36:2201–2206.
28. Oriuchi N, Mamura M, Shibazaki T, et al. Clinical evaluation of thallium-201 SPECT in supratentorial gliomas: relationship to histologic grade, prognosis and proliferative activity. *J Nucl Med* 1993;34:2085–2089.
29. Britten JS, Blamk M. Thallium activation of the (Na+-K+) activated ATPase of rabbit kidney. *Biochem Biophys Acta* 1968;159:160–166.
30. Sessler MJ, Geck P, Maul FD, et al. New aspects of cellular mechanism of ion uptake: K+Na+-2Cl-cotransport is the central mechanism of ion uptake. *Nuklearmedizin* 1986;25:24–27.
31. Muranaka A. Accumulation of radioisotopes with tumor affinity. II. Comparison of the tumor accumulation of Ga-67 citrate and thallium-201 chloride in vitro. *Acta Med Okayama* 1981;35:85–101.
32. Inokuma T, Tamaki N, Torizuka T, et al. Value of fluorine-18-fluorodeoxyglucose and thallium-201 in the detection of pancreatic cancer. *J Nucl Med* 1995;36:229–235.
33. Buchpiguel CA, Alavi JB, Alavi A, Kenyon LC. PET versus SPECT in distinguishing radiation necrosis from tumor recurrence in the brain. *J Nucl Med* 1995;36:159–164.
34. Kahn D, Follett KA, Bushnell DL, et al. Diagnosis of recurrent brain tumor: value of ^{201}Tl SPECT vs. ^{18}F fluorodeoxyglucose PET. *Am J Roentgenol* 1994;163:1459–1465.
35. Oriuchi N, Tomiyama K, Inoue T, et al. Independent thallium-201 accumulation and fluorine-18-fluorodeoxyglucose metabolism in glioma. *J Nucl Med* 1996;37:457–462.
36. Hoh CK, Khanna S, Harris GC, et al. Evaluation of brain tumor recurrence with Tl-201 SPECT studies: correlation with FDG PET and histological results [Abstract]. *J Nucl Med* 1992;33:867.
37. Kubota K, Matsuzawa T, Ito M, et al. Lung tumor imaging by positron emission tomography using C-11-L-methionine. *J Nucl Med* 1985;26:37–42.
38. Lowe VJ, Hoffman JM, Delong DM, Patz EF, Coleman RE. Semiquantitative and

visual analysis of FDG PET images in pulmonary abnormalities. *J Nucl Med* 1994;35:1771–1776.
39. Mori K, Yokoi K, Saito Y, Tominaga K, Miyazawa N. Diagnosis of mediastinal lymph node metastases in lung cancer. *Jpn J Clin Oncol* 1992;22:35–40.
40. Keyes JW. SUV: standard uptake or silly useless value? *J Nucl Med* 1995;36:1836–1839.
41. Tonami N, Yokoyama K, Shuke N, et al. Evaluation of suspected malignant pulmonary lesions with ^{201}Tl single-photon emission computed tomography. *Nucl Med Commun* 1993;14:602–610.
42. Suga K, Kume N, Orihashi, N, et al. Difference in ^{201}Tl accumulation on single photon emission computed tomography in benign and malignant thoracic lesions. *Nucl Med Commun* 1993;14:1071–1078.
43. Orihashi N, Mita T, Uchisaka H, Suga K, Matsumoto T, Nakanishi T. Tl-201 SPECT in the evaluation of small nodular lesions of lung. *Jap J Clin Radiol* 1994;39:159–163.
44. Martin WH, Delbeke D, Patton JA, Sandler MP. Detection of malignancies with SPECT versus PET, with 2-[Fluorine-18]fluoro-2-deoxy-D-glucose. *Radiology* 1996; 198:225–231.
45. Drane WE, Abbott FD, Nicole MW, Mastin ST, Kuperus JH. Technology for FDG SPECT with a relatively inexpensive gamma camera. *Radiology* 1994;191:461–465.
46. Macfarlane DJ, Cotton L, Ackermann RJ, et al. Triple-head SPECT with 2-[fluorine-18] fluoro-2-deoxy-D-glucose (FDG): initial evaluation in oncology and comparison with FDG PET. *Radiology* 1995;194:425–429.
47. Slosman DO, Pugin J. Lack of correlation between tritiated deoxyglucose, thallium-201 and technetium-99m-MIBI cell incorporation under various cell stresses. *J Nucl Med* 1994;35:120–126.
48. Kubota R, Kubota K, Yamada S, et al. Active and passive mechanisms of [fluorine-18]fluorodeoxyglucose uptake by proliferating and prenecrotic cancer cells in vivo: a microautoradiographic study. *J Nucl Med* 1994;35:1067–1075.
49. Higashi K, Clavo AC, Wahl RL. Does FDG uptake measure proliferative activity of human cancer cells? In vitro comparison with DNA flow cytometry and tritiated thymidine uptake. *J Nucl Med* 1993;34:414–419.

Technetium-99m-Labeled Anti-EGF-Receptor Antibody in Patients with Tumor of Epithelial Origin: I. Biodistribution and Dosimetry for Radioimmunotherapy

Normando Iznaga-Escobar, Leonel A. Torres, Alejo Morales, Mayra Ramos, Ivette Alvarez, Niuvis Pérez, Roberto Fraxedas, Oscar Rodríguez, Nelson Rodríguez, Rolando Pérez, Agustín Lage and Michael G. Stabin
Centers of Molecular Immunology, Clinical Research and Medical-Surgical Research, Institute of Nephrology, Orthopedic Hospital Frank País, Havana, Cuba; and Radiation Internal Dose Information Center, Oak Ridge, Tennessee

Accurate estimation of biodistribution and absorbed dose to normal organs and tumors is important for immunoscintigraphic studies and radioimmunotherapy treatment planning. **Methods:** Four patients (3 men, 1 woman; mean age 54.8 ± 9.2 yr; range 42–64 yr) were administered 3 mg of anti-human epidermal growth factor receptor (anti-hEGF-r) antibody (ior egf/r3), radiolabeled with ^{99m}Tc activity of 39.5 ± 1.1 mCi (range 38.5 mCi–40.7 mCi) by intravenous bolus infusion. After administration, blood and urine samples were collected from three patients up to 24 hr after injection. Whole-body anterior and posterior scans were obtained at 5 min and 1, 3, 5 and 24 hr after injection. Using a computer program, regions of interest were drawn over the heart, liver, spleen, bladder and tumor to measure the activity in the source organs at each scanning time. Time-activity curves for each source organ were then fitted to monoexponential or biexponential functions by nonlinear least squares regression using the flexible polyhedrals method, which adequately fit our data with the correlation coefficient of 0.985 ± 0.013, and were integrated to determine organ residence times. The mean absorbed doses to the whole body and various normal organs were then estimated from residence times and from blood and urine samples using the methods developed by the Medical Internal Radiation Dose Committee. The effective dose equivalent and effective dose were calculated as prescribed in ICRP Publication Nos. 30 and 60. **Results:** Plasma disappearance curves of ^{99m}Tc-labeled anti-hEGF-r antibody were best-fit by a two-compartment model in all patients with a distribution half-life ($t_{1/2\alpha}$) of 0.207 hr ± 0.059 hr (mean ± s.d., n = 3) and an elimination half-life ($t_{1/2\beta}$) of 13.9 hr ± 2.2 hr. Among the various organs, significant accumulation of the radiolabeled antibody was found in the liver (48.5% ± 4.4%, mean ± s.d.), heart (3.50% ± 0.17%) and spleen (3.1% ± 1.8%) at 5 min postadministration. These values were reduced to 3.2% ± 0.4%, 0.1% ± 0.01% and 0.1% ± 0.1%, respectively, at 24 hr. Mean cumulative urinary excretion of ^{99m}Tc-labeled anti-hEGF-r antibody was 4.6% ± 0.6% at 24 hr postinjection. Estimates of radiation absorbed dose to normal organs in rad/mCi administered (mean ± s.d., n = 4) were: whole body 0.017 ± 0.002; gallbladder wall 0.074 ± 0.007; spleen 0.136 ± 0.076; and liver 0.267 ± 0.036. The effective dose equivalent and effective dose estimates for adults were 0.041 ± 0.008 rem/mCi and 0.027 ± 0.004 rem/mCi administered. **Conclusion:** This feasibility study indicates that ^{99m}Tc-labeled anti-hEGF-r antibody (ior egf/r3) can be used safely; this analysis provides a dosimetric framework for future studies. This monoclonal antibody, labeled with ^{188}Re, could possibly permit a successful regional radioimmunotherapy of tumors of epithelial origin.

Key Words: biodistribution; dosimetry; radioimmunotherapy; human epidermal growth factor

J Nucl Med 1998; 39:15–23

The technique for the production of monoclonal antibodies (MAbs) of predefined specificity (*1*) resulted in a dramatic increase in the application of radiolabeled antibodies for radioimmunodiagnosis (RAID) and radioimmunotherapy (RAIT). Numerous clinical trials using radiolabeled MAbs for tumor detection, biodistribution and internal radiation dosimetry have been conducted in recent years (*2–4*). Significant positive results have now been achieved in RAID (*5,6*) and RAIT (*7–11*).

The calculation of the absorbed dose has been important in nuclear medicine. Such dose estimates are used to determine the health risks involved and the amount of radionuclides that should be administered to patients during routine procedures. The current Medical Internal Radiation Dose (MIRD) formalism (*12,13*) for estimating doses to individual organs usually includes the assumption of uniform radionuclide distribution in homogeneous media. Although this assumption is not strictly valid in many cases, its use in evaluating internal dose estimates for safety purposes remains routine.

The antibody ior egf/r3, developed at the Center of Molecular

Received Oct. 22, 1996; revision accepted Mar. 19, 1997.
For correspondence or reprints contact: Normando Iznaga-Escobar, Center of Molecular Immunology, P.O. Box 16040, Havana, 11600, Cuba.